ISSN 1674-1056
http://cpb.iphy.ac.cn
http://iopscience.iop.org/cpb
中国物理 B
Chinese Physics
中国物理
Chinese Physics B

Effect of scanning speeds on electrochemical corrosion resistance of laser cladding TC4 alloy

Xiaotian Feng(冯晓甜), Jianbo Lei(雷剑波), Hong Gu(顾宏), Shengfeng Zhou(周圣丰)

Citation: Chin. Phys. B . 2019, 28(2): 026802. **doi:** 10.1088/1674-1056/28/2/026802
Journal homepage: http://cpb.iphy.ac.cn; http://iopscience.iop.org/cpb

What follows is a list of articles you may be interested in

Direct characterization of boron segregation at random and twin grain boundaries

Xiang-Long Li(李向龙), Ping Wu(吴平), Rui-Jie Yang(杨锐杰), Shi-Ping Zhang(张师平), Sen Chen(陈森), Xue-Min Wang(王学敏), Xiu-Lan Huai(淮秀兰)

Chin. Phys. B . 2017, 26(8): 086802. **doi:** 10.1088/1674-1056/26/8/086802

Tensile properties of phase interfaces in Mg–Li alloy：A first principles study

Zhang Cai-Li, Han Pei-De, Wang Xiao-Hong, Zhang Zhu-Xia, Wang Li-Ping, Xu Hui-Xia

Chin. Phys. B . 2013, 22(12): 126802. **doi:** 10.1088/1674-1056/22/12/126802

Effect of scanning speeds on electrochemical corrosion resistance of laser cladding TC4 alloy*

Xiaotian Feng(冯晓甜), Jianbo Lei(雷剑波)†, Hong Gu(顾宏)‡, and Shengfeng Zhou(周圣丰)

Laser Technology Institute, Tianjin Polytechnic University, Tianjin 300387, *China*

(Received 1 October 2018; revised manuscript received 13 December 2018; published online 25 January 2019)

In order to study the effect of scanning speed on the electrochemical corrosion resistance of laser cladding TC4 alloy in artificial seawater, the x-ray diffraction analysis, microstructure of cross-section, microhardness variation, and impedance spectrum have been studied in comparison with the TC4 titanium alloy. The results show that the main phase of cladding coating is α-Ti, and the change of scanning speed has no obvious effect on it; therefore, the supersaturated α-Ti solid solution is formed, and the acicular α' martensite is obtained. As the scanning speed increases, the microstructure of cladding coating is orthogonal basket-weave, the crystal surface spacing decreases, and the average microhardness of laser cladding TC4 alloy slightly increases. When the scanning speed increases to 10 mm/s, the microhardness is about 14.71% higher than that of the substrate, and the electrochemical corrosion resistance of laser cladding TC4 alloy is also improved, which is about 2.48 times more than the substrate. Grain refinement has a great effect on enhancing the anti-electrochemical corrosion.

Keywords: laser cladding, TC4 alloy, grain refinement, electrochemical corrosion

PACS: 68.35.bd, 82.45.Bb **DOI:** 10.1088/1674-1056/28/2/026802

1. Introduction

Titanium alloy has excellent corrosion resistance, high strength, and good fatigue resistance. It is considered to form a stable, continuous oxide film protection on the metal surface. It is also an important structural metal developed in the 1950s and is widely used in aerospace, automotive, and biomedical fields.[1] However, it's easy for titanium alloy parts to have an environment failure of bad situation. For example, corrosion damage,[2] stress corrosion cracking,[3] being paroxysmal, and uncertainty, which limits the application and development of titanium alloys to a large extent. In order to further improve the corrosion resistance and oxidation resistance of titanium alloy, surface treatment of titanium alloy is an effective way to extend its application and development. Generally, there are some surface treatment methods of titanium alloy, such as electroplating, electroless plating, surface oxidation treatment,[4] and so on; however, there are some shortcomings, such as complex technology, high cost, and the electrolytes that are not friendly to the environment.[5–8] On the contrary, laser cladding technology, as a new material surface modification and parts processing technology, has short preparation time and stable quality, and could improve the wear-resisting, corrosion resistant, heat resistant, antioxidant, and other properties of coating surface; it can also eliminate the problem of possible cracks caused by thermal effects.[9–11]

The laser cladding technology of titanium alloy surface is quite mature. Generally speaking, most of the cladding materials are nickel-base,[12–15] cobalt-base,[16–18] iron-base alloy,[19–21] and tungsten carbide composite materials.[22–25] Among metal powders, the research and application of the fusible alloy powder are the most. Lu *et al.*[26] and Weng *et al.*[27] reported Ni-based composite coatings and Co-based composite coatings prepared by laser cladding on Ti-6Al-4 V, respectively. They found that both composite coatings had good metallurgical combination with no porosity and crack, and the microhardness and wear resistance have also been further improved, which is due to the fact that the hard phase (TiC, TiB_2, *etc.*) and enhanced phase were formed on the coating. However, the corrosion resistance and the electrochemical corrosion properties of cladding coating were not presented in their study, and it would make sense to study its anti-electrochemical corrosion performance. Amado *et al.*[28] also used laser cladding technology to prepare the Ni-WC coating with different WC gradient contents, and they observed that the longitudinal composite gradient of a millimetre can be obtained along the laser scanning direction. As we can see, there are many studies about various laser cladding materials on titanium alloy surface, which indicates that the laser cladding technology is undoubtedly a good way to explore the unknown properties of the material.

Statistically, the microstructure and mechanical properties of laser cladding TC4 alloy have been extensively

*Project supported by the National Natural Science Foundation of China (Grant Nos. 61475117 and 51471084), the National Key Research and Development Program of China (Grant No. 2017YFB1103604), and the Tianjin Municipal Special Program of Talents Development for Excellent Youth Scholars, China (Grant No. TJTZJHQNBJRC-2-15).

†Corresponding author. E-mail: ljbtj@163.com

‡Corresponding author. E-mail: guhong1120@163.com

© 2019 Chinese Physical Society and IOP Publishing Ltd

investigated,[29–33] but few studies have explored the electrochemical corrosion properties of laser cladding TC4 alloy. Therefore, this paper mainly studies the microstructure and electrochemical corrosion properties of laser cladding TC4 alloy.

2. Experiment

2.1. Experimental materials and equipment

TC4 titanium alloy (Ti-6Al-4V) was selected as substrate, and the machining dimension was 60 mm×60 mm×20 mm. The cladding material was TC4 alloy powder. Table 1 gives the composition of Ti-6Al-4V alloy powder. Obviously, Ti was the main component.

Table 1. Composition of TC4 alloy (wt%).

Contents	Ti	Al	V	Fe	C	N	H	O
TC4	Bal.	5.5–6.8	3.5–4.5	≤0.3	≤0.1	≤0.05	≤0.015	≤0.20

LDM-8060-type high power semiconductor laser made in Nanjing Zhongke Raychan was used for the laser cladding of multi-channel single-layer TC4 alloy on the substrate with different scanning speeds of 4 mm/s, 7 mm/s, and 10 mm/s. Figure 1 shows the working schematic of laser cladding, and several laser process parameters in this paper were as follows: 2 kW of laser power, 50% of overlap rate, coaxial powder cladding, and protected by argon gas.

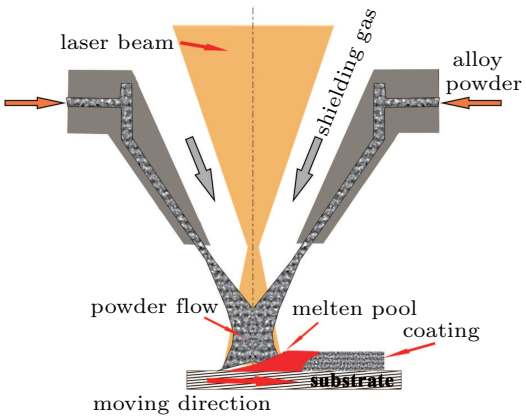


Fig. 1. The working schematic of laser cladding.

2.2. Performance testing

The microhardness was measured by HXDG1000T-type digital microhardness tester; 0.2-kg load and 10-s load stay times were selected. A point was made every 50 μm from the proximity of the coating surface in the sample section, all in the same line, and tested three times on average.

The electrochemical corrosion resistance was tested by CHI606E electrochemical workstation of Shanghai Chenhua. Electrolyte was 3.5-wt% NaCl solution, using three-electrode measuring system, including auxiliary electrode (platinum electrode), reference electrode (saturated silver chloride electrode), and working electrode (the sample coating). The area of working electrode surface was 1 cm^2, and the frequency range of electrochemical impedance test was 10^{-2} Hz–10^5 Hz. Before testing the sample coating, we put them in electrolyte solution for 1 hour; all tests were completed under the open-circuit potential of stability test, and then electrochemical impedance spectroscopy was tested and dynamic potential polarization curve is scanned from −1.2 V to 1.2 V of corrosion potential with a scanning rate of 20 mV/min. Sometimes, corrosion current density on the surface of the electrode might be mutated because of the generation and rupture of bubbles, which would affect the quality of the dynamic potential polarization curves, so solutions should be de-aerated, and bubbles should be avoided as much as possible during the experiment. Simultaneously, the self-corrosion potential and self-corrosion current density of the cladding coating in the corrosion process were calculated by CHI606E software, and the electrochemical impedance spectrum was analysed by ZSimpWin software; the corresponding equivalent circuit was also found. Last but not least, the above electrochemical tests were averaged at least three times.

2.3. Microstructure characterization

The x-ray diffraction (XRD) was used to analyze the phase structure of the coating, scanning from 10° to 80° of 2 thetas. And the microstructure of the coating was observed by Sigma300 field emission scanning electron microscope (SEM). Besides, the ratio of the etching solution was hydrofluoric acid: nitric acid: distilled water = 1:2:59; corrosion time was 30 s.

3. Results discussion and analysis

3.1. Characterization of laser cladding coating

Figure 2(a) shows the microstructure of laser cladding Ti-6Al-4V alloy. It can be seen that its microstructure is composed of fine acicular α-martensite and original β-grain boundary, and fine acicular α phase is titanium over saturated acicular martensite. Chen *et al.*[34] found this rule and conducted qualitative analysis of sample phase composition by x-ray diffraction, indicating that the main phase of laser cladding TC4 alloy was close-packed hexagonal lattice of α-Ti solution. The phase composition of cladding coating under different scanning speeds has been analysed by XRD analysis, as shown in Fig. 2(b). It is found that the main phase of cladding coating is α-Ti, and the change of scanning speed has no obvious influence on it, but the x-ray diffraction peaks show a slight right shift phenomenon. As the scanning speed

increases, the peak value is slightly enhanced, the lattice constants of the laser cladding TC4 alloy are smaller, and the crystal surface spacing decreases.[34] This is because the atomic radius of the solvent atom Ti is slightly larger than that of the solute atom Al and V; when the solute atom and the solvent lattice are miscible, the lattice contraction is easily to occur, and thus the lattice constant is reduced. As it is further cooled from the β phase, it will lead to the α phase nucleation in the original β-crystalline boundary and grow to the original β-crystalline interior along the determined bit. It is further indicated that the solid solubility of the α-Ti solid solution increases with the laser beam in the process of melting the TC4 alloy powder, and it is a non-equilibrium rapid melting and solidification process during the laser beam irradiation on the TC4 alloy powder.[35] Moreover, based on the heat transfer characteristics of the molten pool itself, the enriched solute atoms in the interface of the molten pool are "captured" and solidified by the high-speed moving interface before they are fully diffused,[31] thus α-Ti solid solution is formed, and the acicular martensite is obtained.

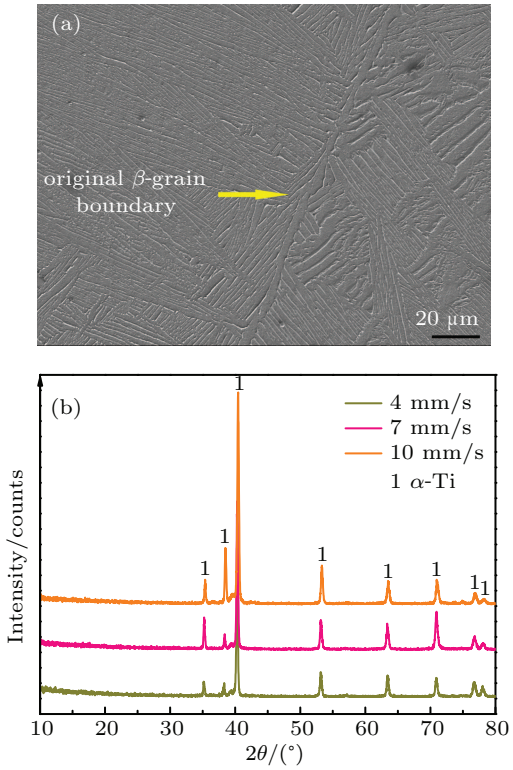


Fig. 2. (a) The SEM image of laser cladding TC4 alloy; (b) x-ray diffraction patterns.

Figures 3(a), 3(c), and 3(e) show the microstructure of bonding zone of laser cladding TC4 alloy. There is no obvious crack and pore in the bonding zone, which indicates that the substrate and cladding layer have good metallurgical bonding. It can be seen that the microstructure of heat affected zone (HAZ) is significantly different from that of the substrate. The substrate (TC4 titanium alloy) is a type of $\alpha+\beta$ alloy, which is shown in the box of Fig. 3(a), with a typical basket-weave and a grain size of 1 μm–1.2 μm. Compared with the substrate, the grain size of laser cladding TC4 alloy becomes thinner, which is 0.3 μm–0.5 μm. When the molten pool reaches the supercooling degree, β columnar crystals are formed first, and the α phase nucleates and grows up at the β grain boundary. However, due to the high laser energy density and rapid cooling rate, the alloying elements on both sides of the solid and liquid interfaces in the molten pool have solidified before they have time to diffuse.[36] Thereby, an α-Ti solid solution is formed, resulting in fine acicular α' martensite.

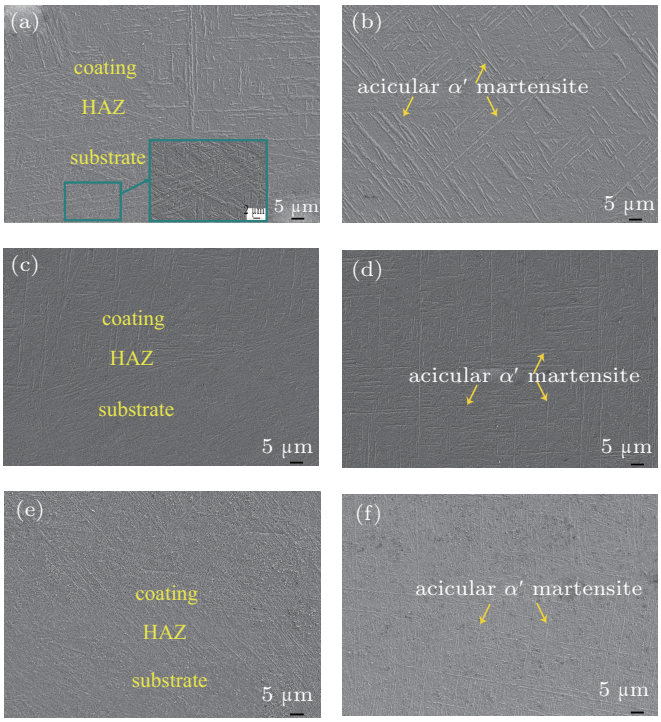


Fig. 3. Microstructure morphology of the cross section with different scanning speeds: (a) and (b) 4 mm/s, (c) and (d) 7 mm/s, and (e) and (f) 10 mm/s. (a), (c), and (e) bonding zone; (b), (d), and (f) middle.

In addition, as shown in Figs. 3(b), 3(d), and 3(f), the middle of microstructure of laser cladding TC4 alloy is different as the scanning speed increases. It can be seen that when the laser power remains constant and the scanning speed is 4 mm/s, the acicular α' martensite is slightly thicker, and the size of the formed basket weave is different. At 7 mm/s, acicular α' martensite becomes slightly thinner, but its microstructure is not uniform. At 10 mm/s, the microstructure exhibits a very uniform orthogonal basket-weave, and the acicular α' martensite becomes finer.

3.2. Microhardness analysis

Figure 4(a) shows the comparison of microhardness distribution of laser cladding TC4 alloy and substrate under different scanning speeds. It can be seen that the microhardness of all the three cladding coatings is higher than that of

substrate; when the scanning speed is increased to 10 mm/s, the microhardness is about 14.71% higher than that of the substrate. What is more, the average microhardness of laser cladding TC4 alloy with different scanning speeds is shown in Fig. 4(b). It can be seen that as the scanning speed increases, the average microhardness of cladding coating slightly increases, and the average microhardness of the substrate is about 340 $HV_{0.2}$.

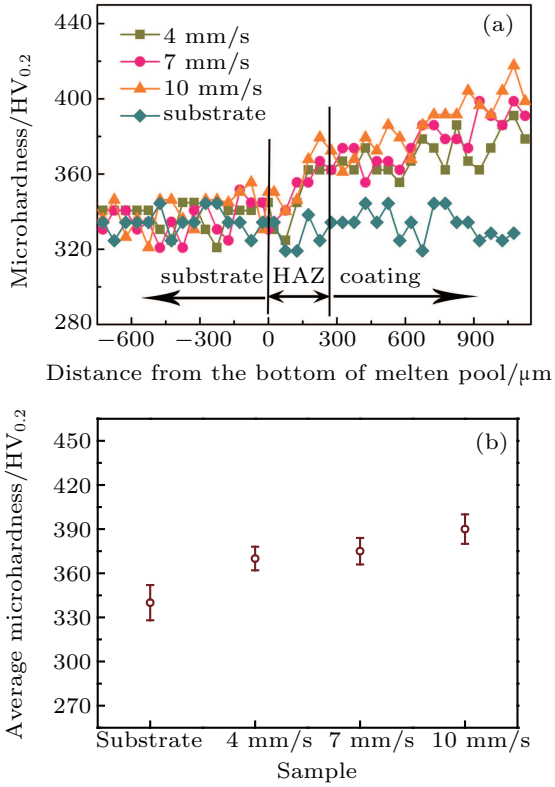


Fig. 4. (a) Microhardness distribution; (b) average microhardness.

The high cooling rate during laser cladding process could also enhance the microhardness of cladding coating. For a simple quantitative analysis, the temperature of the molten pool during laser cladding process can be calculated as follows:[37,38]

$$T(x,y,z) = T_0 + \frac{\alpha P}{\pi^{3/2} kr} \int_0^{\infty} \frac{1}{1+S^2} \exp\left\{ -\frac{S^2}{1+S^2} \times \left[\left(\frac{x}{r} - \frac{ar}{2S^2} \right)^2 + \left(\frac{y}{r} \right)^2 \right] - S^2 \left(\frac{z}{r} \right)^2 \right\} \mathrm{d}s, \quad (1)$$

where T_0 is the preheated temperature of substrate, the absorption coefficient of the substrate α was 0.71, $a = \rho cv/k$, the thermal conductivity coefficient k is 6.8 W/(m·K), the density ρ is 4450 kg/m^3, and the thermal capacity c is 611 J/(kg·K).[39] The radius of laser spot r is 2 mm, the laser power P is 2 kW, and the scanning speed v is from 4 mm/s to 10 mm/s. The temperature gradient G_T can be described as follows:[38]

$$G_T = \frac{\partial T}{\partial z}. \quad (2)$$

The calculated temperature gradient and cooling rate of the molten pool during laser cladding process are shown in Fig. 5. As the scanning speed increases, the temperature gradient G_T decreases as shown in Fig. 5(a), and the cooling rate increases as shown in Fig. 5(b), the solidification rate R increases, the ratio of G_T and R is small, and the degree of supercooling is big. Because the microstructure of cladding coating is affected by the degree of supercooling of the component during the laser cladding process, the grain size is relatively fine as shown in Fig. 3(c). Thus, the average microhardness of the laser cladding TC4 alloy is relatively increased, which represents that the dendrite refinement enhances the strength of the cladding coating.[40]

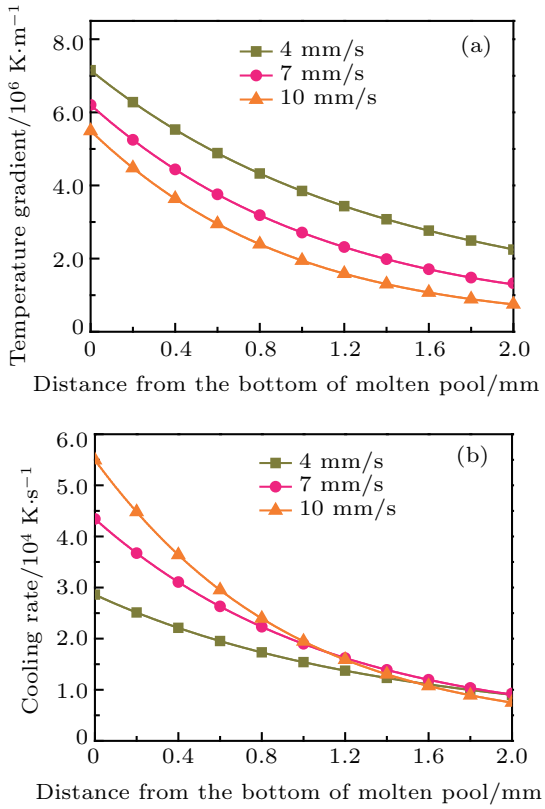


Fig. 5. (a) Temperature gradient; (b) cooling rate.

As the depth to the heat affected zone increases, the temperature gradient G_T of cladding coating increases, the solidification rate R decreases, the ratio of G_T to R increases, the degree of supercooling decreases, and the grain size becomes larger from about 0.3 μm to 1 μm; hence the microhardness inside the heat affected zone gradually decreases.

3.3. Electrochemical corrosion performance

3.3.1. Dynamic potential polarization curve

The dynamic potential polarization curves of laser cladding TC4 alloy and substrate (Sub) are tested with 3.5% NaCl solution of electrolyte for three different scanning speeds (L1: 4 mm/s, L2: 7 mm/s, and L3: 10 mm/s) at room temperature, as shown in Fig. 6.

As we can see, as the corrosion voltage in the anode region increases, the corrosion current of cladding coating and the substrate is significantly increased. The specimen surface is in an active dissolving state. The characteristics of the polarization curves of cladding coating and the substrate are compared, which shows that both of their passivation behaviour is obvious.[41] Compared with the substrate, laser cladding TC4 alloy has higher self-corrosion potential, lower corrosion current density, and lower passivation current density. And when entering the passivation zone, the voltage increases, and the corrosion current is almost unchanged, indicating that the cladding layer is in a passivation state; this is because the oxide film on the surface inhibits further dissolution of the coating. In addition, in the last half of the slow increase in voltage, it can be seen that the corrosion current is also slowly increasing, and the oxide film is gradually dissolved. As the Cl^- ions in electrolyte pass through the oxide film, the Ti elements of cladding coating are dissolved, accordingly Ti^{2+} increases and the hydrolysis reaction occurs[42,43]

$$\mathrm{Ti} \rightarrow \mathrm{Ti}^{2+} + 2\mathrm{e}, \tag{3}$$

$$\mathrm{Ti}^{2+} + 2\mathrm{H_2O} \rightarrow \mathrm{Ti(OH)_2} + 2\mathrm{H}^+. \tag{4}$$

The PH value of electrolyte is reduced and the conditions for further dissolution of titanium are provided.

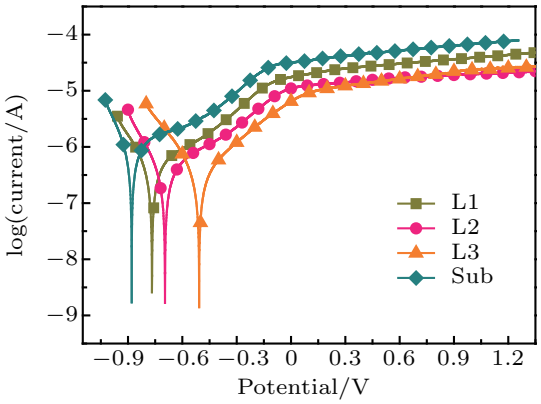


Fig. 6. The potential dynamic polarization curves.

In the cathode region, it can be observed that as the voltage increases, the current drops sharply, indicating an oxygen reduction reaction occurs[44]

$$\mathrm{O_2} + 4\mathrm{H}^+ + 4\mathrm{e} = 2\mathrm{H_2O}. \tag{5}$$

Some chemical parameters such as corrosion potential E_{corr}, corrosion current density i_{corr}, and polarization resistance R_p can be obtained from dynamic potential polarization curves, as shown in Table 2. It can be concluded that as the scanning speed increases, the self-corrosion potential E_{corr} of laser cladding TC4 alloy becomes more and more positive, and corrosion current density i_{corr} gradually decreases. Compared with the other two groups of scanning speed and substrate, when the scanning speed is 10 mm/s, it has the maximum polarization resistance, indicating the best corrosion resistance of this cladding coating.

Table 2. The standard corrosion parameters of polarization curve.

Material	E_{corr}/V	i_{corr}/μA·cm^{-2}	β_a	β_c	R_p/Ω
4 mm/s	–0.768	0.3862	3.688	6.012	115019
7 mm/s	–0.696	0.2968	3.942	6.467	140783
10 mm/s	–0.507	0.2512	4.602	6.729	159086
Substrate	–0.892	0.7743	3.728	7.360	50641

Moreover, polarization linear resistance is also a kinetic parameter for measuring electrode corrosion rate.[45] The greater the polarization linear resistance, the smaller the self-corrosion current density, and the better the corrosion resistance of material. The self-corrosion resistance is

$$R_p = \frac{B}{i_{corr}}, \quad B = \frac{\beta_a \beta_c}{\beta_a + \beta_c}, \tag{6}$$

where β_a is the slope of the Tafel anode curve, and β_c is the slope of the Tafel cathode curve.[46] And the corrosion rate v_{corr} can be calculated by the following equation:[47]

$$v_{corr} = \frac{0.00327 \times EW. \times i_{corr}}{\rho}, \tag{7}$$

where 0.00327 is a constant that defines the unit of the corrosion rate (in unit mm/y), the i_{corr} is the corrosion current density (in units μA·cm^{-2}), ρ is the specimen density, and EW is the equivalent of the alloy which can be calculated by the following equation:

$$EW = \frac{1}{\sum \left[\frac{n_i \times f_i}{W_i} \right]}, \tag{8}$$

where f_i is the weight fraction of the i-th element of the alloy, and W_i and n_i are the atomic weight and valence states of the i-th element of the alloy, respectively.[47]

By calculation, the magnitude of corrosion rate is in the order of the scanning speed of 10 mm/s < 7 mm/s < 4 mm/s < substrate, which concludes that the corrosion rate is determined by the corrosion current density, which also indicates that in contrast, when the scanning speed is 10 mm/s, it has the lowest corrosion rate and the best corrosion resistance.

3.3.2. AC impedance spectrum

As shown in Fig. 7(a), the AC impedance spectra of the specimens can exist in the form of Nyquist plots. In the literature,[48] it was mentioned that in electrochemical corrosion, Nyquist plots were composed of the real and imaginary parts of the impedance. The larger the radius of the resistance arc, the better the corrosion resistance of material. It is visible in Fig. 7(a) that as the scanning speed increases, the radius of the resistance arc increases, which represents that the corrosion resistance of TC4 alloy coating is enhanced. And laser cladding TC4 alloy coating has better corrosion resistance than the substrate.

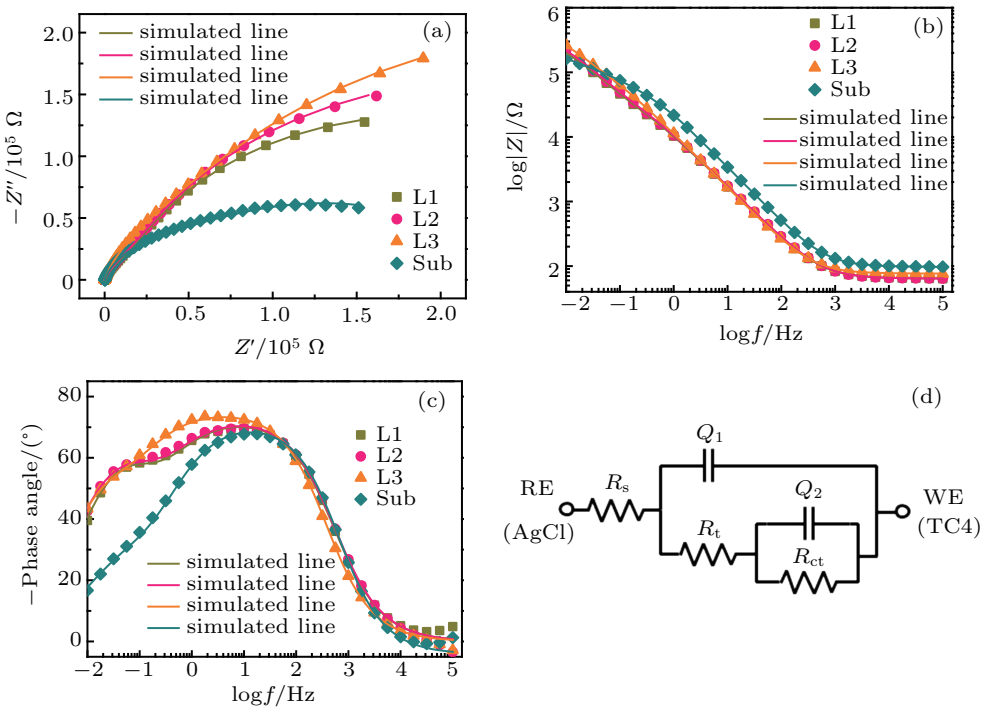


Fig. 7. EIS results: (a) Nyquist plot; (b) and (c) Bode diagrams; (d) equivalent circuit model.

In addition, as shown in Figs. 7(b) and 7(c), AC impedance spectra exist in the form of Bode impedance and Bode phase angle diagrams. It can be seen that for the laser cladding TC4 alloy with different scanning speeds, when the applied frequency f increases, both the impedance $|Z|$ and phase angle are relatively increased. Compared with the substrate, when the scanning speed is 10 mm/s, the phase angle is relatively large in the range of low-frequency to middle-frequency, which illustrates that the laser cladding TC4 alloy has high capacitance behaviour, and the dense oxide film is formed on the coating surface.[49] Thus, this explains that the laser cladding TC4 alloy has the best electrochemical corrosion resistance when the scanning speed is 10 mm/s.

As shown in Fig. 7(d), laser cladding TC4 alloy and substrate have the same equivalent circuit model, which can be used to measure the impedance data.[50] The equivalent circuit model consists of an electrolyte solution resistance R_s, a resistance R_t caused by surface defects of coating, a charge transfer resistance R_{ct}, and two constant phase-angle elements Q_1 and Q_2, both of which involve two parameters: $Y_0 > 0$ and dispersion index $0 < n < 1$.[51] During the electrochemical corrosion process, a dense protective layer forms on the coating in the electrolyte, enhances the resistance of the oxide film, increases the corrosion resistance, and thus slows down the corrosion rate of the coating, and enhances the corrosion resistance, which is consistent with the results of the dynamic polarization curve. Furthermore, the corresponding electrical parameters are obtained from the EIS data, as shown in Table 3. It clearly shows that the charge transfer resistance R_{ct} of laser cladding TC4 alloy coating is larger than that of the substrate; when the scanning speed is 10 mm/s, it has the largest charge transfer resistance R_{ct} (4.203×10^5 $\Omega\cdot cm^{-2}$), which is about 2.48 times larger than the substrate (1.694×10^5 $\Omega\cdot cm^{-2}$). The dispersion exponent n also reflects the density of the formed oxide film; it can be observed that when the scanning speed is 10 mm/s, a more compact oxide film is formed. Finally, the standard error of measurement is less than 3%,[51] which represents that this experimental data and the simulated data agree well. In addition, it is also consistent with the decrease of the crystal surface spacing and the increase of microhardness of the laser cladding TC4 alloy, indicating that with the increase of the scanning speed, the crystal surface spacing of cladding coating gradually decreases, which is also one of the important reasons for its improvement of electrochemical corrosion resistance.

Table 3. Electrical parameters of the equivalent circuits.

No.	$R_s/\Omega\cdot cm^{-2}$	$(Q_1$–$Y)/\Omega^{-1}\cdot s^{-n}\cdot cm^{-2}$	n_1	$R_t/10^5$ $\Omega\cdot cm^{-2}$	$(Q_2$–$Y)/\Omega^{-1}\cdot s^{-n}\cdot cm^{-2}$	n_2	$R_{ct}/10^5$ $\Omega\cdot cm^{-2}$	Std. error/%
L1	63.94	$2.016.\times10^{-5}$	0.818	0.581	$1.914.\times10^{-5}$	0.825	3.042	<1.749
L2	63.95	$1.944.\times10^{-5}$	0.820	0.610	$1.664.\times10^{-5}$	0.782	3.929	<1.898
L3	76.42	$1.872.\times10^{-5}$	0.841	1.580	$1.880.\times10^{-5}$	0.760	4.203	<1.626
Sub	93.41	$1.037.\times10^{-5}$	0.802	0.418	$0.645.\times10^{-5}$	0.731	1.694	<2.195

3.3.3. Mechanism analysis after corrosion

Figures 8(a) and 8(b) show the microstructure of cladding coating with scanning speed of 4 mm/s and substrate after potential polarization corrosion. It can be concluded that the corrosion zone of the substrate (in red region) is relatively large, and the corrosion zone of cladding coating is comparatively small. Due to the minor defects on the surface of the sample coating, the area of defects is small and the metal potential is low, which can become an anode. When the corrosion current is highly concentrated to the defects, corrosion rapidly develops as pitting corrosion in defects. After the pitting corrosion is formed, once the oxygen is consumed, it further becomes the anode of the oxygen concentration battery, and the corrosion progress in the pitting is accelerated. In addition, the surface near the pitting corrosion is protected by the cathodic reduction reaction, and the corrosion further develops in the pitting. It illustrates that the laser cladding TC4 alloy has better electrochemical corrosion resistance than the substrate.

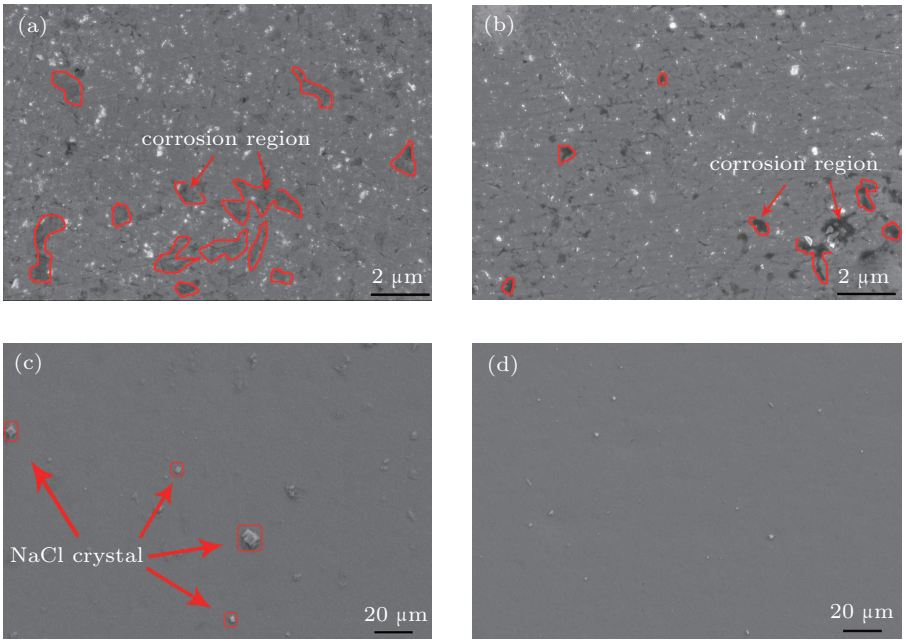


Fig. 8. The SEM images after electrochemical corrosion: (a) substrate; (b) 4 mm/s; (c) 7 mm/s; (d) 10 mm/s.

Similarly, figures 8(c) and 8(d) respectively show the microstructure of cladding coating with a scanning speed of 7 mm/s and 10 mm/s after potential polarization corrosion. The small squares pointed by the red arrows in Fig. 8(c) should be the precipitated NaCl crystals, in the cubic shape. It can be seen that with the increase of the scanning speed, the precipitation on the surface of cladding coating becomes more homogeneous and finer. Compared with the untreated substrate, there is no obvious corrosion area, which is consistent with the increasing trend of R_{ct} in Table 3; therefore, it states that the corrosion resistance of the laser cladding TC4 alloy is much better.

4. Conclusions

In this paper, the TC4 alloy coatings are fabricated by laser cladding technology on the TC4 titanium alloy plate; the microstructure, microhardness, and electrochemical corrosion resistance of laser cladding TC4 alloy are analysed, which are concluded as follows:

(i) The microstructure of laser cladding TC4 alloy is composed of fine acicular α-martensite and original β-grain boundary, generating α-Ti solid solution and obtaining uniform orthogonal basket-weave. As the scanning speed increases, the acicular α' martensite becomes thinner and denser, the strength of the x-ray diffraction peak of cladding layer is enhanced and the peak is slightly right shifted, the lattice constants of the laser cladding TC4 alloy become smaller, and the crystal surface spacing is decreased. And there are no obvious cracks and pores in the bonding zone, which illustrates that the substrate and cladding layer have good metallurgical bonding.

(ii) The average microhardness of laser cladding TC4 alloy is higher than that of the substrate, and as the scanning speed increases, the microhardness of cladding coating is slightly improved; when the scanning speed increases to 10 mm/s, the microhardness is about 14.71% higher than that of the substrate; in addition, dendrite refinement enhances the microhardness of laser cladding TC4 alloy.

(iii) Compared with the substrate, as the scanning speed increases, the self-corrosion potential E_{corr} of cladding coating becomes more and more positive, the capacitive arc radius in the Nyquist plots is also increased, and the Bode impedance and phase angle are relatively increased, which indicates that

the electrochemical corrosion resistance of the laser cladding TC4 alloy is improved. It is also proved that with the increase of the scanning speed, the decrease of crystal surface spacing is also an important reason for improving the electrochemical corrosion resistance.

(iv) Compared with the substrate, the corrosion zone of laser cladding TC4 alloy is significantly reduced after the potential polarization corrosion, and with the increase of the scanning speed, the precipitation on the surface of cladding coating becomes even finer.

References

[1] Polmear I, StJohn D, Nie J F and Qian M 2017 *Light Alloys*, 5th edn. (Boston: Butterworth-Heinemann) pp. 369–460

[2] Shoesmith D W, Noël J J and Annamalai V E 2016 *Corrosion of Titanium and Its Alloys* in*: Reference Module in Materials Science and Materials Engineering* (Elsevier)

[3] Cao S, Zhu S M, Samuel Lim C V, Zhou X G, Chen X B, Hinton B R W, Boyer R R, Williams J C and Wu X H 2017 *Corrs. Sci.* **125** 29

[4] Li C G, Wang B, Pan B, Huang W H and Wang Y 2015 *Hot Work. Technol.* **44** 22 (in Chinese)

[5] Sibileva S V, Botanogov A L, Trofimov N V and Zaharova L V 2015 *Adv. Mater. Res.* **1101** 4

[6] Critchlow G W, Brewis D M 1995 *Int. J. Adhes Adhes* **15** 161

[7] Mertens T, Gammel F J, Kolb M, Rohr O, Kotte L, Tschoecke S, Kaskel S and Krupp U 2012 *Int. J. Adhes Adhes* **34** 46

[8] Rico-Oller B, Mertens T, Kolb M, Wehr J and Zheludkevich M L 2016 *Mater. Sci. Eng. Technol.* **47** 400

[9] Yuan Q L, Feng X D, Cao J J and Su Z J 2010 *Mater. Rev.* **24** 112 (in Chinese)

[10] Chikarakara E, Naher S and Brabazon D 2012 *Surf. Coat. Technol.* **206** 3223

[11] Dong C S, Gu Y, Zhong M L, Ma M X, Huang T and Liu W J 2012 *Acta Phys. Sin.* **61** 094211 (in Chinese)

[12] Zhang K M, Zou J X, Li J, Yu Z S and Wang H P 2012 *T. Nonferr. Met. Soc.* **22** 1817

[13] Yan X J, Gugel H, Huth S and Theisen W 2011 *Mater. Lett.* **65** 2934

[14] Lei J B, Shi C, Zhou S F, Gu Z J and Zhang L C 2018 *Surf. Coat. Technol.* **334** 274

[15] Zhao Z, Chen J, Tan H, Lin X and Huang W D 2017 *Opt. Laser Technol.* **92** 36

[16] Weng F, Yu H J, Chen C Z, Liu J L, Zhao L J and Dai J J 2016 *J. Alloys Compd.* **686** 74

[17] Weng F, Yu H J, Chen C Z and Dai J J 2015 *Mater. Design* **80** 174

[18] Majumdar J D 2011 *Adv. Mater. Sci. Eng.* **2011** 2237

[19] Wang S L, Zhang Z Y, Gong Y B and Nie G M 2017 *J. Alloys Compd.* **728** 1116

[20] Gong F B, Shen J, Gao R H, Zhang T, Xie X and Yang L 2016 *T. Nonferr. Met. Soc.* **26** 2117

[21] Chen J M, Guo C and Zhou J S 2012 *T. Nonferr. Met. Soc.* **22** 2171

[22] Zhou S F and Zeng X Y 2010 *J. Alloys Compd.* **505** 685

[23] Wang X Y, Zhou S F, Dai X Q, Lei J B, Guo J B, Gu Z J and Wang T 2017 *Int. J. Refract. Met. Hard Mater.* **64** 234

[24] Ma Q S, Li Y J, Wang J and Liu K 2015 *J. Alloys Compd.* **645** 151

[25] Li G J, Li J and Luo X 2014 *Mater. Charact.* **98** 83

[26] Lu X L, Liu X B, Yu P C, Qiao S J, Zhai Y J, Wang M D, Chen Y and Xu D 2016 *Opt. Laser Technol.* **78** 87

[27] Weng F, Yu H J, Chen C Z, Liu J L and Zhao L J 2015 *J. Alloys Compd.* **650** 178

[28] Amado J M, Montero J, Tobar M J and Yáñez A 2014 *Phys. Procedia* **56** 269

[29] Chen J, Zhang S Y, Xue L, Yang H O, Lin X and Huang W D 2007 *Rare Met. Mater. Eng.* **36** 475 (in Chinese)

[30] Sun Y W and Hao M Z 2012 *Opt. Laser Eng.* **50** 985

[31] Wen R J, Tan H, Zhang F Y, Chen J and Huang W D 2012 *Appl. Laser* **32** 91 (in Chinese)

[32] Weng F, Chen C Z and Yu H J 2014 *Mater. Des.* **58** 412

[33] Li G R, Wang F F, Wang H M, Zheng R, Xue F and Cheng J F 2017 *Chin. Phys. B* **26** 046201

[34] Chen J, Yang H O, Yang J and Huang W D 2004 *Mater. Chin.* **23** 33 (in Chinese)

[35] Lin X, Xue L and Chen J 2009 *Chin. Surf. Eng.* **22** 19

[36] Zhang S Y, Lin X , Chen J, Zhang F Y and Huang W D 2007 *Rare Met. Mater. Eng.* **36** 1839

[37] Li Y S, Wu X C, Liu W, Hou Z Y and Mei H J 2015 *Chin. Phys. B* **24** 126401

[38] Picasso M, Marsden C F, Wagniere J D, Frenk A and Rappaz M 1994 *Metall. Mater. Trans. B* **25** 281

[39] Zhang S 2015 "Fabrication and Numerical Simulation of Cobalt-based Composite Coating on Titanium Alloy Surface by Laser Caldding", MS dissertation (Dalian: Dalian University of Technology of China) (in Chinese)

[40] Xu H Y, Zhang W, Fan K and Fu P F 2017 *Rare Met. Mater. Eng.* **46** 1457

[41] Chen J and Zhang Q 2016 *T. Nonferr. Met. Soc.* **26** 1011

[42] Bolzan J A, Jauregui E A and Arvia A J 1963 *Electrochim. Acta* **8** 589

[43] Schmuckler J S 1981 *J. Chem. Edu.* **58** 404

[44] Sato N 2011 *Green Corrosion Chemistry and Engineering*, Sharma S K Ed. (Weinheim: Wiley-VCH) pp. 1–32

[45] Hu P, Song R, Li X J, Deng J, Chen Z Y, Li Q W, Wang K S, Cao W C, Liu D X and Yu H L 2017 *J. Alloys Compd.* **708** 367

[46] Cao C N 2008 *Corros Sci. Prot Technol.* **3** 165 (in Chinese)

[47] Walker R 1993 *Mater. Design* **14** 207

[48] Sulima I, Kowalik R and Hyjek P 2016 *J. Alloys Compd.* **688** 1195

[49] Cheng J, Li F, Zhu S Y, Yu Y, Qiao Z H and Yang J 2017 *Tribol. Int.* **115** 483

[50] Lin C H and Duh J G 2009 *Surf. Coat. Technol.* **204** 784

[51] Liao C J, Yang J S, He Y H and Ming X Z 2015 *J. Alloys Compd.* **619** 221